

The performance of the Noblesse multi-collector noble gas mass spectrometer for $^{40}\text{Ar}/^{39}\text{Ar}$ geochronology

Defeng He¹  · Finlay M. Stuart^{1,2} · Dan N. Barfod³ · Fang Xiao¹ · Hong Zhong¹

Received: 19 December 2017 / Revised: 10 January 2018 / Accepted: 2 February 2018
© Science Press, Institute of Geochemistry, CAS and Springer-Verlag GmbH Germany, part of Springer Nature 2018

Abstract Noblesse multi-collector noble gas mass spectrometer is specially designed for multi-collection of Ar isotopes with different beam sizes, especially for small ion beams, precisely, and hence is perfectly suitable for $^{40}\text{Ar}/^{39}\text{Ar}$ geochronology. We have analyzed widely used sanidine, muscovite, and biotite standards with recommended ages of ~ 1.2 –133 Ma, with the aim to assess the reliability of Noblesse for $^{40}\text{Ar}/^{39}\text{Ar}$ dating. An ESI MIR10 30W CO₂ laser was used for total fusion or incremental heating samples. Extracted gases were routinely purified by four SAES NP10 getters (one at ~ 400 °C and others at room temperature). A GP50 getter and a metal cold finger cooled by liquid N (-196 °C) were also attached for additional purification if necessary. The Ar isotopes were then measured by Noblesse using Faraday or multiplier according to the signal intensities. Over a period of 1.5 months 337 air calibrations produced a weighted mean $^{40}\text{Ar}/^{36}\text{Ar}$ of 296.50 ± 0.08 (2σ , MSWD = 4.77). Fish Canyon sanidine is used to calculate J-values, which show good linear relationship with position in irradiation. The age of four mineral standards (Alder Creek sanidine,

Brione muscovite, Yabachi sanidine, and Fangshan biotite) are within error of the accepted ages. Five Alder Creek sanidine aliquots yielded an age range of 1.174 – 1.181 ± 0.013 Ma (2σ) which broadly overlaps the established age of the standard and the uncertainty approaches those of the foremost Ar/Ar laboratories in the world. The weighted mean ages of four Brione muscovite aliquots (18.75 ± 0.16 Ma, 2σ), five Yabachi sanidine aliquots (29.50 ± 0.19 Ma, 2σ), and three Fangshan biotite aliquots (133.0 ± 0.76 Ma, 2σ) are consistent with the recommended values of these standards, and the uncertainties are typical of modern Ar/Ar laboratories worldwide.

Keywords Ar/Ar geochronology · Multi-collector · High precision · Noblesse · Age standard

1 Introduction

The $^{40}\text{Ar}/^{39}\text{Ar}$ dating method is arguably the most widely applied and precise methods of geochronology. It is predicated on the radioactive decay of ^{40}K to ^{40}Ar and has largely superseded the K–Ar technique (Merrihue and Turner 1966; McDougall and Harrison 1999). The K–Ar method, as originally formulated, relies on direct measurement of K and Ar abundances in two separate splits of a dateable material. This approach is limited by a number of potential factors including sample inhomogeneity, initial excess argon, and Ar-loss and -gain after cooling below the Ar closure temperature. The $^{40}\text{Ar}/^{39}\text{Ar}$ dating technique is based on the conversion of ^{39}K to ^{39}Ar in samples by neutron activation (n, p reaction) in a nuclear reactor. The ^{39}Ar abundance serves as a proxy for ^{40}K (requires assumption about the $^{40}\text{K}/^{39}\text{K}$ ratio) and permits the

Electronic supplementary material The online version of this article (<https://doi.org/10.1007/s11631-018-0265-8>) contains supplementary material, which is available to authorized users.

✉ Defeng He
hedefeng@vip.gyig.ac.cn

¹ State Key Laboratory of Ore Deposit Geochemistry, Institute of Geochemistry, Chinese Academy of Sciences, 99 Linchengxi Road, Guiyang 550081, China

² Isotope Geoscience Unit, Scottish Universities Environmental Research Centre, East Kilbride G75 0QF, UK

³ NERC Argon Isotope Facility, Scottish Universities Environmental Research Centre, East Kilbride G75 0QF, UK

simultaneous measurement of both the parent and daughter nuclide in a single argon isotope measurement. A standard mineral (monitor) with an independently determined age is used to precisely calculate the amount of ^{39}K that has been converted to ^{39}Ar . The monitors are evenly distributed amongst the irradiated sample so that the neutron fluence (^{39}K production rate, J) can be calculated at a given sample position. Subsequent $^{40}\text{Ar}/^{39}\text{Ar}$ measurements for an unknown sample can then be used to calculate age.

Ar isotope determinations for $^{40}\text{Ar}/^{39}\text{Ar}$ geochronology are typically determined using single-collector magnetic sector and mass spectrometers. Data collection is performed using a “peak-jumping” procedure where the magnetic field strength or the ion acceleration potential is changed to focus the individual Ar isotopes onto a single collector. A new generation of multiple-collector magnetic sector mass spectrometers have been developed for $^{40}\text{Ar}/^{39}\text{Ar}$ dating. One design uses five Faraday detectors equipped with 10^{11} and 10^{12} Ω resistors (GV Instruments ARGUS V; Mark et al. 2009). A variant of this instrument includes a low mass electron multiplier (Thermo Scientific ARGUS VI; Kim and Jeon 2015; Phillips et al. 2017; Bai et al. 2018). The Nu-Instruments Noblesse mass spectrometer has an array of ion-counting electron multipliers for Ar isotope abundance determinations (Cosca 2007; Coble et al. 2011; Jicha et al. 2010, 2016). The third mass spectrometer has an array of five movable detectors, which can each be switched between an ion-counting electron multiplier and a Faraday cup (GV Instruments HELIX-MC and Thermo Scientific HELIX-MC plus, Marrocchi et al. 2009; Zhang et al. 2016). Isotopic ratio measurement using multi-collector mass spectrometers have better precision than single collector instruments, and they dramatically reduce the size of samples that are necessary for $^{40}\text{Ar}/^{39}\text{Ar}$ analysis. They also increase sample throughput and permit more robust analytical strategies, such as better background and discrimination control, replicate analyses, etc. In this contribution we describe the Nu instruments Noblesse mass spectrometer that is located in the State Key Laboratory of Ore Deposit Geochemistry, Institute of Geochemistry Chinese Academy of Sciences (IGCAS), and we review its performance.

2 Mass spectrometer description

The Nu instruments Noblesse mass spectrometer is a single focusing magnetic sector instrument with a 75° angle flight tube, two ion-optic lens arrays and a Nier-type ion source. The focusing of the ion beam and collector-slit spacing produce broad, flat-topped peaks with steep sides that afford improved resolution compared to the previous generation of single-collector instruments. The Nu Noblesse at

IGCAS has a sensitivity of 14.0 A/mol Ar in static mode using the Faraday detector. The analytical volume of 2229 ± 22 mL includes SAES NP10 getters mounted on source and detector blocks. A Faraday cup (FAC) with 10^{11} Ω resistor occupies the high mass position, while three secondary electron multipliers (ETP) operating in ion-counting (IC) mode are fixed in an array designated IC0, IC1, and IC2 (from high to low mass). Electrostatic filters are located at the entrance of the IC1 and IC2 detectors in order to suppress scattered ions. Background levels of Ar in the extraction-purification system (isolated for 5 min) are typically 5.5×10^{-16} mol ^{40}Ar , 9.8×10^{-19} mol ^{39}Ar , 1.1×10^{-18} mol ^{38}Ar , 1.7×10^{-17} mol ^{37}Ar , 4.4×10^{-18} mol ^{36}Ar . Blanks that completely simulate the analysis procedure are measurably higher: 7.5×10^{-16} , 5.0×10^{-17} , 1.7×10^{-18} , 1.9×10^{-17} , and 7.6×10^{-18} mol for ^{40}Ar through ^{36}Ar .

The mass resolving power (MRP), or the ability of the instrument to resolve isobaric interferences, is defined as $m/\Delta m$, where m is the peak mass and Δm is the mass difference between 5% and 95% peak height as determined by the side of the peak (Ireland 2013). The IGCAS Noblesse has MRP that is typically 2200–2800. This does not allow for the resolution of the interferences produced by HCl^+ and hydrocarbon species that are present at the high mass side of the Ar peaks. This is especially important for $^{12}\text{C}_3^+$ and H^{35}Cl^+ at mass 36. Peak heights are measured on the least affected low-mass peak sides, and these are accounted for by equivalent measurements in the blank.

An ultra-high vacuum gas purification line is directly attached to the mass spectrometer. Calibration gases are contained in two gas reservoirs that include pipettes for producing reproducible gas amounts. Gas is extracted either using an ESI MIR10 30W CO_2 laser or a double-walled vacuum furnace. The gas released from samples is purified by exposure to two SAES NP10 getters. A metal cold finger cooled by liquid N (-196°C) and a GP50 getter are used for “dirty” samples, such as whole rock basalts. Single crystals (e.g. sanidine, mica) can be fused with the laser, and ~ 1 –5 mg of K-bearing minerals can be heated incrementally. Samples are melted in a single step using laser power of 5–6 W for 30 s. For incremental heating extraction, the sample is irradiated by the laser beam in approximately ten steps ranging from 0.6 to 6 W for 90 s in a raster scan mode. The active gases are consumed by the NP10 getters for 5 min. One getter is held at $\sim 400^\circ\text{C}$ (0.65 A), and the other kept at room temperature. For “dirty” samples, the gas is exposed to the cold finger and the GP50 getter for an additional 5 min. Blanks are measured for every three analyses of samples. Purification procedure and timings are identical to those used for sample analysis. Air standards are measured after every ten analyses in order to determine mass discrimination. The

raw data of blank, air, standard, and sample are input into ArArCalc software (Koppers 2002), and regressed to inlet time. The J-value and sample age are determined from the measured Ar isotope composition after the corrections are made for interfering nuclear reactions, mass discrimination, procedural blanks, and concentration of atmospheric Ar. Each age includes the error assigned to the J parameter, in this case 0.5%.

3 Performance

Typical multi-collection analysis methods for the IGCAS Noblesse are summarized in Table 1. Each method requires unique detector and source settings in order to optimize peak shape and maximize beam intensity (Fig. 1). For analysis of atmospheric Ar, the ^{40}Ar , ^{38}Ar and ^{36}Ar beam intensities are measured simultaneously on the Faraday cup, IC1 and IC2, respectively. For typical $^{40}\text{Ar}/^{39}\text{Ar}$ measurement of samples, ^{40}Ar and ^{39}Ar are usually analyzed on the same detector in peak-jumping mode (for example method 2 and method 4; Table 1) to minimize the influence of IC gain fluctuation during analysis. In order to generate similar beam intensities of ^{40}Ar and ^{39}Ar , irradiation time and sample amounts are carefully calculated according to their potassium contents and estimated ages. Samples with significantly different ^{40}Ar and ^{39}Ar beam intensities require use of the Faraday and IC1, respectively (e.g., method 3; Table 1). The beam intensity ratio intercalibration (BI-IC) method (Turpin and Swisher III 2010), which measures the appropriate ^{40}Ar beam size (3–15 mV) among Faraday and electron multipliers, was applied to determine the IC gains. They were measured before experiments each day and typically reported averages of 0.993 ± 0.002 (IC0), 0.934 ± 0.002 (IC1) and 0.993 ± 0.002 (IC2) for 10 days (1σ , 10 runs from June 8th to 18th, 2017) and showed no correlation with beam size (Fig. 2).

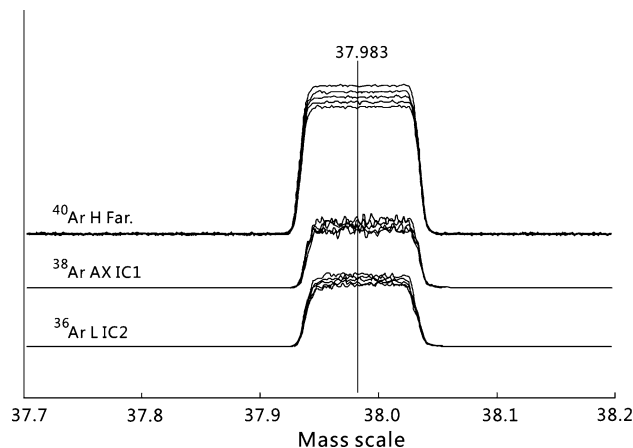


Fig. 1 Peak scans showing peak top and peak side stability during continuous scanning of an air calibration shot (initially ~ 100 mV for ^{40}Ar , 25 s per scan and ~ 135 s interval between 2 scans). Gas consumption within the mass spectrometer accounts for the decreasing beam intensities

4 Air standards

The Ar isotope analysis of a typical air standard is shown in Fig. 3. All beam intensities decreased with time. They showed slight concave upward forms that reflect the consumption of gas by ionization and detection. Exponential lines were fitted, but the Ar isotope ratios showed no obvious change with time. Figure 4a, b show ^{40}Ar (Faraday) and ^{36}Ar (electron multiplier) beam intensities plotted against the precision of measurements. Faraday beam intensities derived from 1.1×10^{-11} mol Ar have a measurement precision of 0.002%. For analysis of 2.1×10^{-14} mol the measurement precision was 0.46%. For the electron multiplier, 3.7×10^{-14} mol Ar was measured with a precision of 0.03% whereas 7.4×10^{-17} mol Ar was measured with a precision of 0.58%. Pipettes of air yielding 7.9×10^{-13} mol ^{40}Ar produced a beam intensity of ~ 110 mV on the Faraday cup that had a precision of 0.02%, while 2.7×10^{-15} mol ^{36}Ar produced $\sim 2.3 \times 10^4$ counts per second (cps) on the

Table 1 Typical multi-collection analysis methods for a Noblesse configured with one Faraday (FAC) and three ion-counting electron multipliers (IC)

Detector	Mass position	Multicollection detector settings							
		Method 1		Method 2		Method 3		Method 4	
Far	High	^{40}Ar	^{40}Ar	^{39}Ar	^{40}Ar	–	–	–	–
IC0	High	–	–	–	–	–	^{40}Ar	^{39}Ar	
IC1	Axial	^{38}Ar	^{38}Ar	^{37}Ar	^{38}Ar	^{39}Ar	^{38}Ar	^{37}Ar	
IC2	Low	^{36}Ar	^{36}Ar	–	^{36}Ar	^{37}Ar	^{36}Ar	–	
Application		Air	> 16 mV ^{40}Ar and ^{39}Ar		> 16 mV ^{40}Ar and < 16 mV ^{39}Ar		< 16 mV ^{40}Ar and ^{39}Ar		

This is similar to methods presented by Coble et al. (2011)

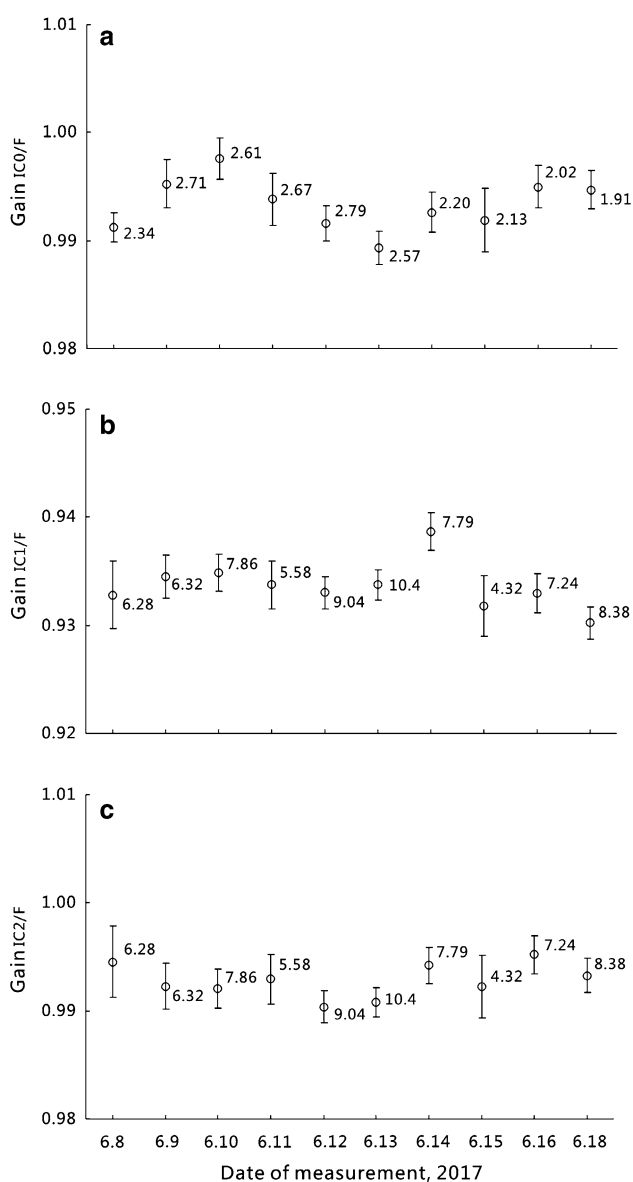


Fig. 2 a–c IC gains with 1 sigma uncertainties measured using (BIC) method (Turrin and Swisher III 2010) remain almost constant within 10 days of sample analysis and exhibit no correlation with beam size. The intensity of ^{40}Ar on Faraday (mV) of each analysis is adjacent to each data point

electron multiplier (equivalent to 0.37 mV on the Faraday) and had a precision of 0.1%.

The $^{40}\text{Ar}/^{36}\text{Ar}$ of 337 air calibrations measured between October 18th and November 30th 2016 have a normal distribution and yield a weighted mean of 296.50 ± 0.08 (Fig. 5; 2σ , MSWD = 4.77). This corresponds to a mass discrimination value of 1.001738 ± 0.000543 , according to the atmospheric argon $^{40}\text{Ar}/^{36}\text{Ar}$ (298.56 ± 0.31 ; Lee et al. 2006).

The effect of Ar partial pressure on source sensitivity and mass fractionation was assessed by the analysis of varying amounts of atmospheric Ar. There was no

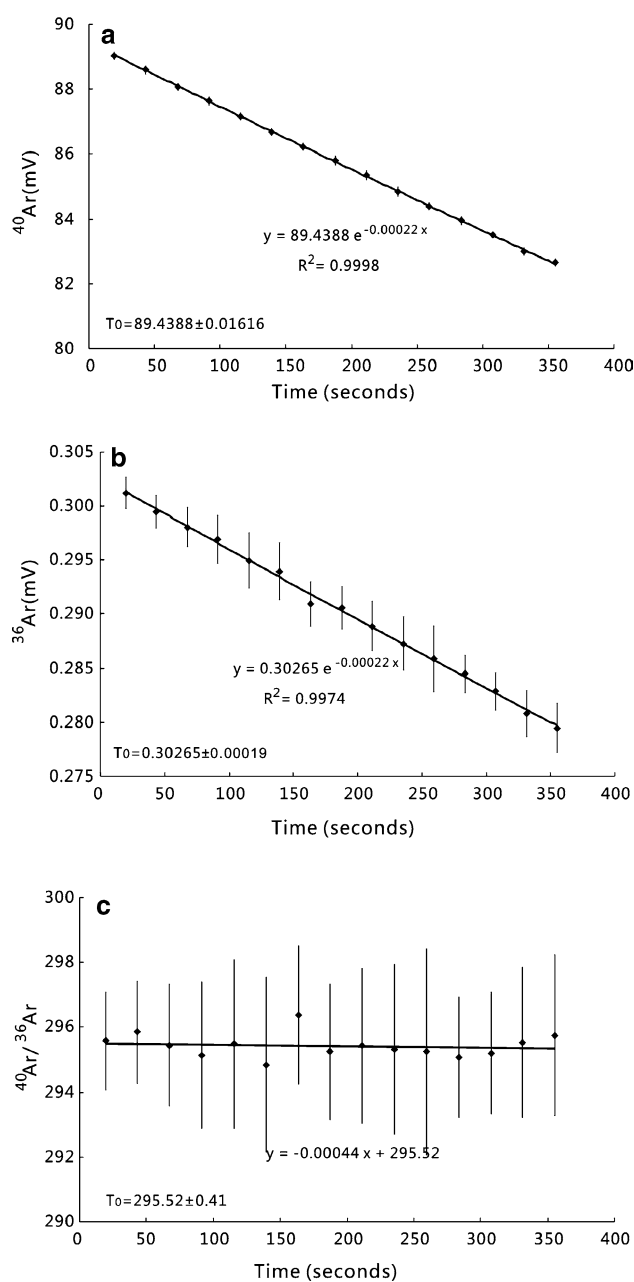


Fig. 3 a Raw ^{40}Ar peak evolution. Data conform to an exponential fit. b Raw ^{36}Ar peak evolution. Data conform to an exponential fit. c Multi-collector $^{40}\text{Ar}/^{36}\text{Ar}$ collected online

resolvable difference in the measured $^{40}\text{Ar}/^{36}\text{Ar}$ ratio by varying the ^{40}Ar signal size from 1538 mV (1.1×10^{-11} mol) to 2.94 mV (2.1×10^{-14} mol; $n = 72$) (Fig. 4c). During analysis of $^{40}\text{Ar}/^{39}\text{Ar}$ mineral age standards, there was no significant control on the $^{40}\text{Ar}/^{39}\text{Ar}$ by signal size. Uncertainty in the determination of $^{40}\text{Ar}/^{36}\text{Ar}$ was governed by the determination of the small ion beam intensities, i.e., ^{36}Ar . For instance, for $^{36}\text{Ar}^+$ beam intensities, uncertainty increased quickly with decreasing beam size below 10^{-15} mol (Fig. 4b).

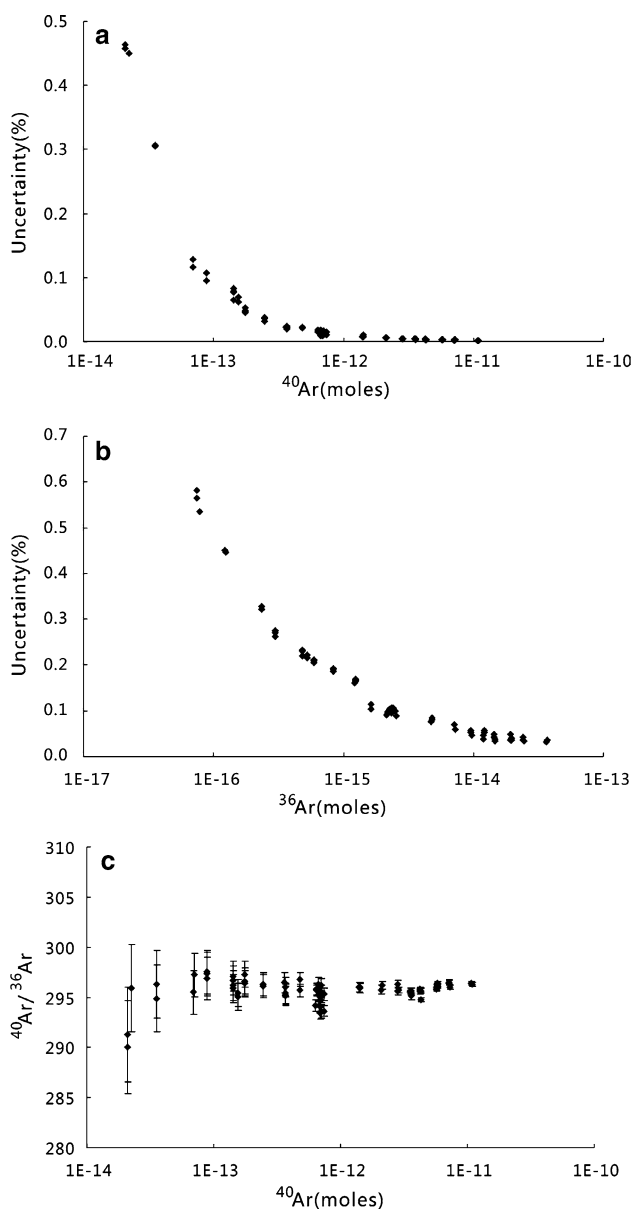


Fig. 4 Plots showing the uncertainty for measurements of varying ion beam size for **a** Faraday, **b** multiplier, and **c** $^{40}\text{Ar}/^{36}\text{Ar}$ linearity with changes in ^{40}Ar signal size. The range in ion beam intensities covers the complete size range for sample ^{40}Ar analyzed at IGCAS

5 Age standards

Here we report data from five well-characterized $^{40}\text{Ar}/^{39}\text{Ar}$ age standards in order to assess the performance of Noblesse. We have analyzed Alder Creek sanidine (ACs; e.g., 1.181 ± 0.001 Ma, Phillips et al. 2017; 1.185 ± 0.001 Ma, Niespolo et al. 2017; 1.185 ± 0.004 Ma, Kim and Jeon 2015; 1.178 ± 0.002 Ma, Phillips and Matchan 2013; 1.185 ± 0.002 Ma, Rivera et al. 2013), Brione muscovite (Bern4M; 18.74 ± 0.20 Ma, Hall et al. 1984), Fish Canyon tuff sanidine (FCs; e.g., 28.126 ± 0.019 Ma, Phillips et al. 2017; 28.01 ± 0.04 Ma, Phillips and Matchan 2013;

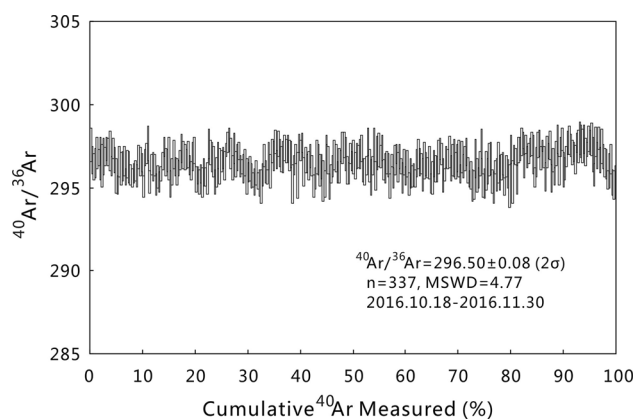


Fig. 5 Measurement of $^{40}\text{Ar}/^{36}\text{Ar}$ ratios of modern atmospheric argon in the laboratory over 1.5 months

28.172 ± 0.028 Ma, Rivera et al. 2011; 28.294 ± 0.036 Ma, Renne et al. 2011; 28.201 ± 0.046 Ma, Kuiper et al. 2008), Yabachi sanidine (YBCs; RYBCs FCs = 1.044296 ± 0.003968 , Wang et al. 2014), Fangshan biotite (ZBH25; 133.0 ± 0.3 Ma, Sang et al. 2006).

All samples were wrapped in Al foil to form ~ 4 mm diameter \times 1 mm thick wafers. The wafers were stacked in quartz vials (Fig. 6) with the Fish Canyon sanidine standard used as the neutron flux monitor. The vial was 25 mm long and had an inner diameter of 5.0 mm. The vials were vacuum-sealed and put inside a quartz canister. The canister was wrapped in 0.5 mm thick Cd foil in order to shield from slow neutrons thus minimize undesirable interference reactions generated during irradiation. The

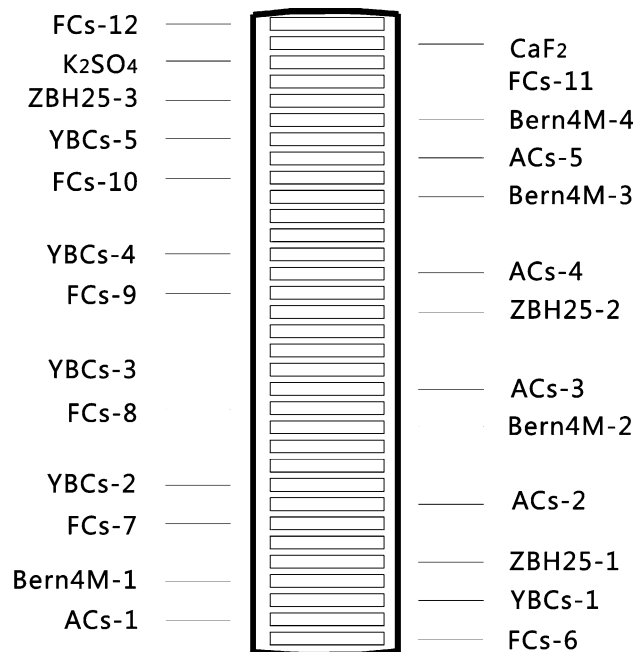


Fig. 6 Packing list of vial II: ACs, FCs, YBCs, Bern4M, ZBH25, K_2SO_4 and CaF_2 in a sealed quartz vial

canister was irradiated in position E4 of the 49-2 Nuclear Reactor (49-2 NR), Beijing for 24 h, with a neutron flux of $2.65 \times 10^{13} \text{ n (cm}^2 \text{ s}^{-1})$. The correction factors for interfering isotopes obtained from the irradiation of pure CaF_2

and potassium salt K_2SO_4 were $(^{39}\text{Ar}/^{37}\text{Ar})_{\text{Ca}} = 1.02 \times 10^{-3}$, $(^{36}\text{Ar}/^{37}\text{Ar})_{\text{Ca}} = 2.69 \times 10^{-4}$, and $(^{40}\text{Ar}/^{39}\text{Ar})_{\text{K}} = 6.64 \times 10^{-3}$, respectively.

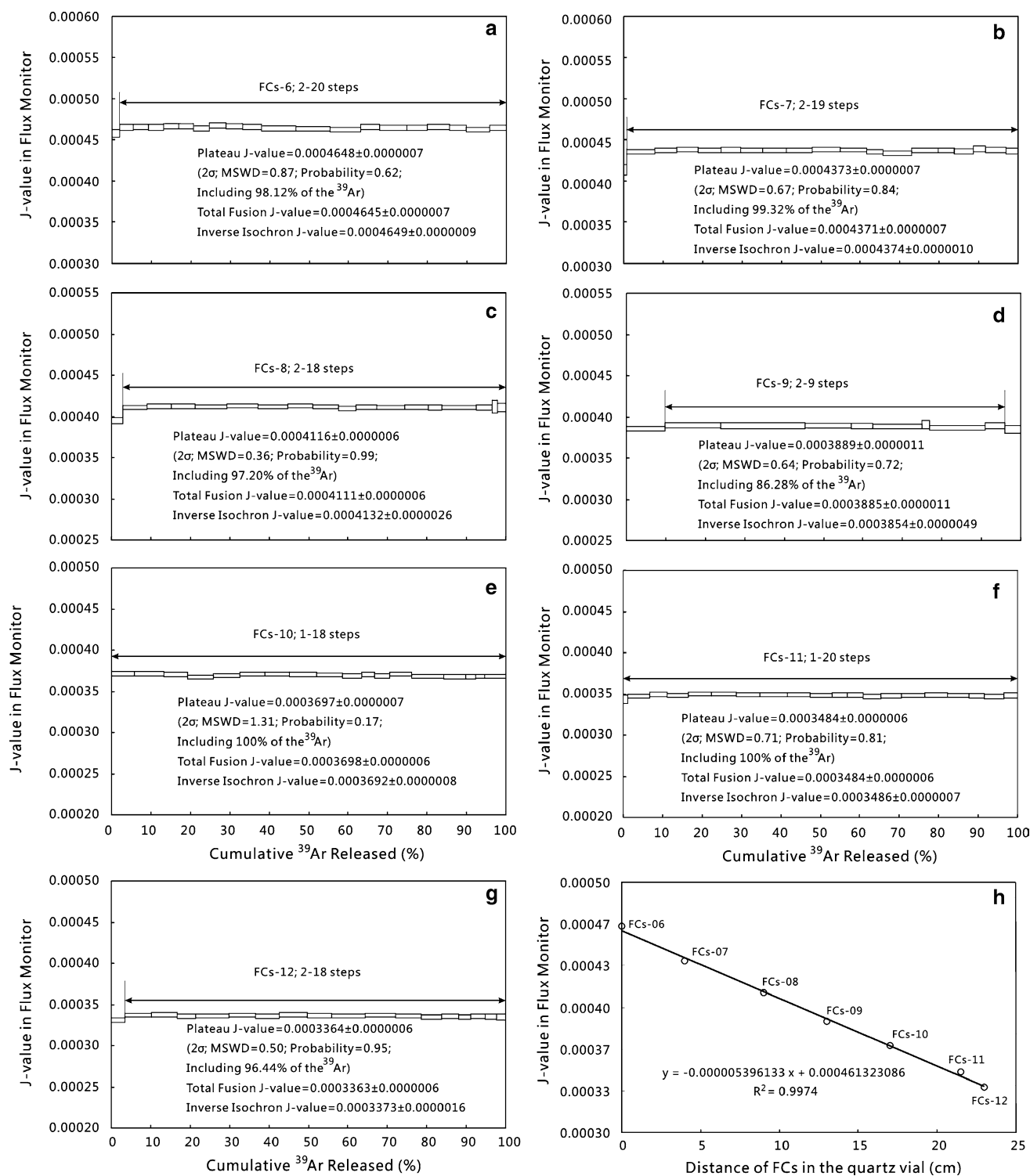


Fig. 7 a–g The J-value step-heating spectra for FCs and the box heights on the plateau diagram reflect the 2σ uncertainties for each step; h vertical flux gradient of standard monitor FCs of vial II

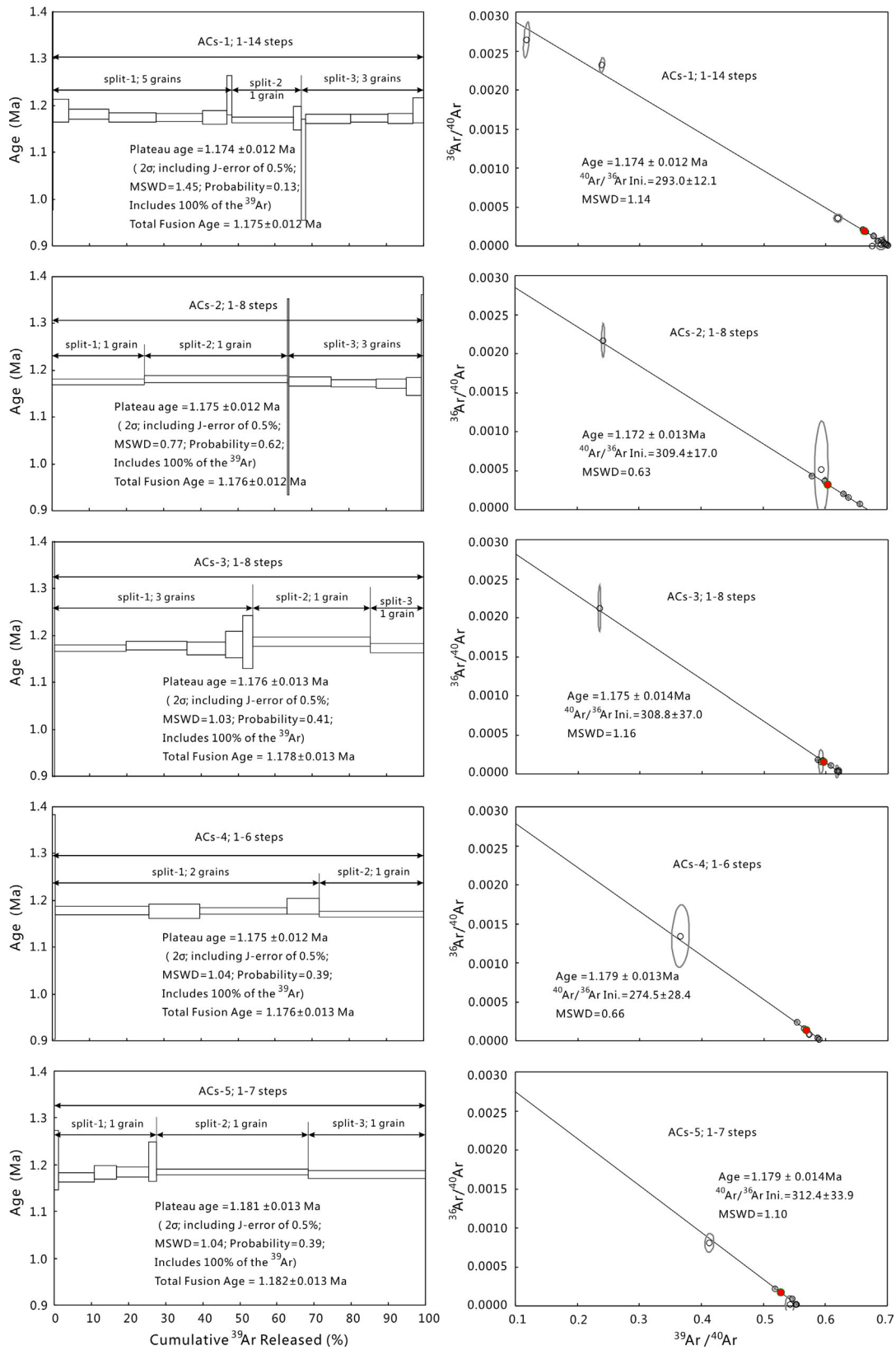


Fig. 8 The $^{40}\text{Ar}/^{39}\text{Ar}$ step-heating spectra and inverse isochrons for ACs. The box heights on the plateau diagram reflect the 2 σ uncertainties for each step

After irradiation, seven FCs aliquots (Fig. 6, denoted FCs-6 to FCs-12) were step-heated to obtain the J-values using the age of 28.294 ± 0.036 Ma (Renne et al. 2011). J-values (Fig. 7a–g) display a nearly linear relationship with position [$y = (-0.000005396133) \times (+0.000461323086)$, $R^2 = 0.9974$; Fig. 7h]. The J-values of the samples were calculated according to their positions. ACs, Bern4M, YBCs, and ZBH25 were analyzed as the same way as FCs. $^{40}\text{Ar}/^{39}\text{Ar}$ age spectra, normal isochrons, inverse isochrons, and total fusion age (TFA) are all within error of each other

for ACs, Bern4M, YBCs, and ZBH25 (Figs. 8, 9, 10, 11). Ages and uncertainties were derived from the $^{40}\text{Ar}/^{39}\text{Ar}$ age spectra of each standard and total fusion analysis in order to directly compare with K–Ar dating of standards.

Step-heating of multi-grain samples (2–5 grains) and total fusion of single crystals were conducted on splits of five aliquots of ACs (Fig. 8, denoted ACs-1 to ACs-5). One split with single grain of aliquot ACs-5 was also analyzed by laser step-heating. The results of single-grain measurements are consistent with those of multi-grain. All

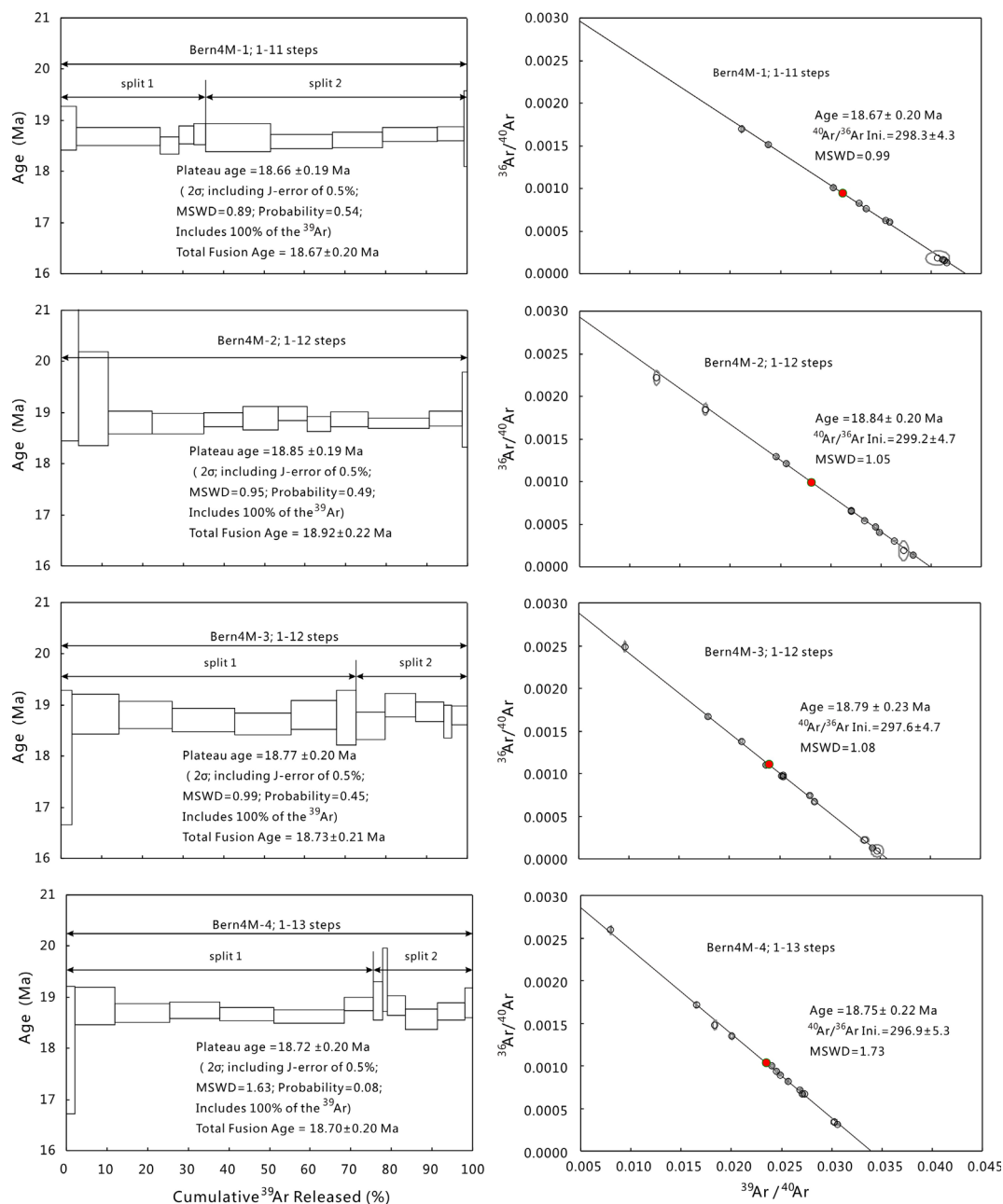


Fig. 9 The $^{40}\text{Ar}/^{39}\text{Ar}$ step-heating spectra and inverse isochrons for Bern4M. The box heights on the plateau diagram represent the 2σ uncertainties for each step

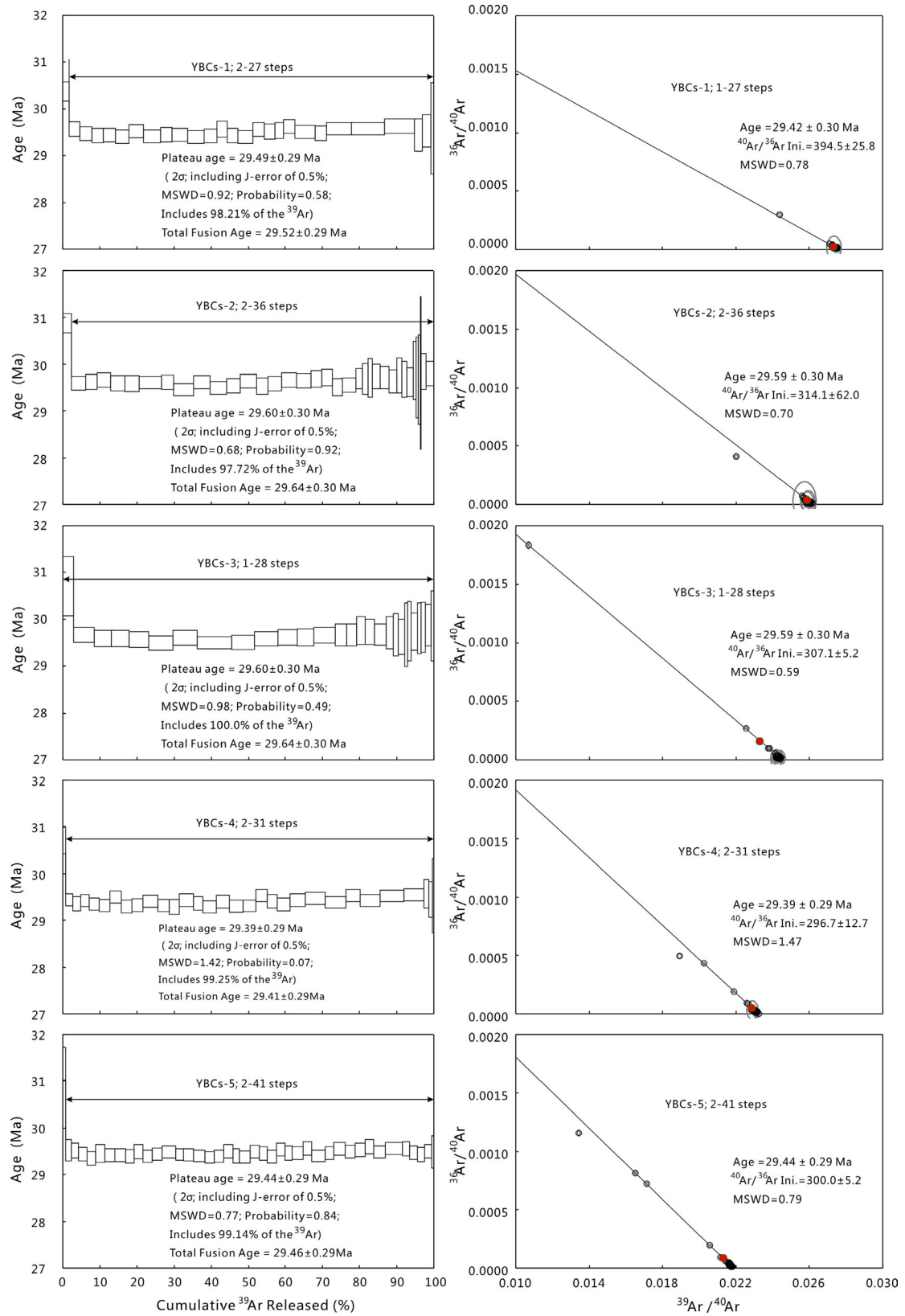


Fig. 10 The ⁴⁰Ar/³⁹Ar step-heating spectra and inverse isochrons for YBCs. The box heights on the plateau diagram represent 2σ uncertainties for each step

analyses yielded an age range of $1.174\text{--}1.181 \pm 0.013$ Ma (2σ , probability = 0.13–0.62, MSWD = 0.77–1.45, TFA = $1.175\text{--}1.182 \pm 0.013$ Ma). This overlapped the established age of the standard (e.g., 1.181 ± 0.001 Ma, Phillips et al. 2017; 1.185 ± 0.001 Ma, Niespolo et al. 2017; 1.185 ± 0.004 Ma, Kim and Jeon 2015; 1.178 ± 0.002 Ma, Phillips and Matchan 2013; 1.185 ± 0.002 Ma, Rivera et al. 2013) and the uncertainty approaches those of the foremost Ar/Ar laboratories in the world.

Four aliquots of Bern4M (Fig. 9, denoted Bern4M-1 to Bern4 M-4) were subjected to laser step-heating analysis. These analyses produced ages of $18.66\text{--}18.85 \pm 0.20$ Ma (2σ , probability = 0.08–0.54, MSWD = 0.89–1.63, TFA = $18.67\text{--}18.92 \pm 0.22$ Ma) and a weighted mean age of 18.75 ± 0.16 Ma (2σ). The ages (inverse isochron, plateau and total fusion age) are within the uncertainty of the accepted age and the error is slight improvement on

previously published data (18.74 ± 0.20 Ma, Hall et al. 1984).

YBC sanidine is from a phonolite of the Yabachi volcanic field in central Tibet, China. It was jointly developed by four laboratories in Australasia and Eurasia for a new standard mineral for $^{40}\text{Ar}/^{39}\text{Ar}$ dating. Based on FCs age of 28.02 ± 0.16 Ma (Renne et al. 1998), the recommended age of YBC sanidine is 29.286 ± 0.206 Ma, or neglecting the decay constant error, 29.286 ± 0.045 Ma (Wang et al. 2014). Detailed laser step-heating experiments of 27–41 steps were carried out on five aliquots of YBC sanidine (Fig. 10, denoted YBCs-1 to YBCs-5). These analyses resulted in ages of $29.39\text{--}29.60 \pm 0.30$ Ma (2σ , probability = 0.07–0.92, MSWD = 0.68–1.42, TFA = $29.41\text{--}29.64 \pm 0.30$ Ma) and a weighted average age of 29.50 ± 0.19 Ma (2σ) relative to a FCs age of 28.294 ± 0.036 Ma (Renne et al. 2011). According to the inter-calibration

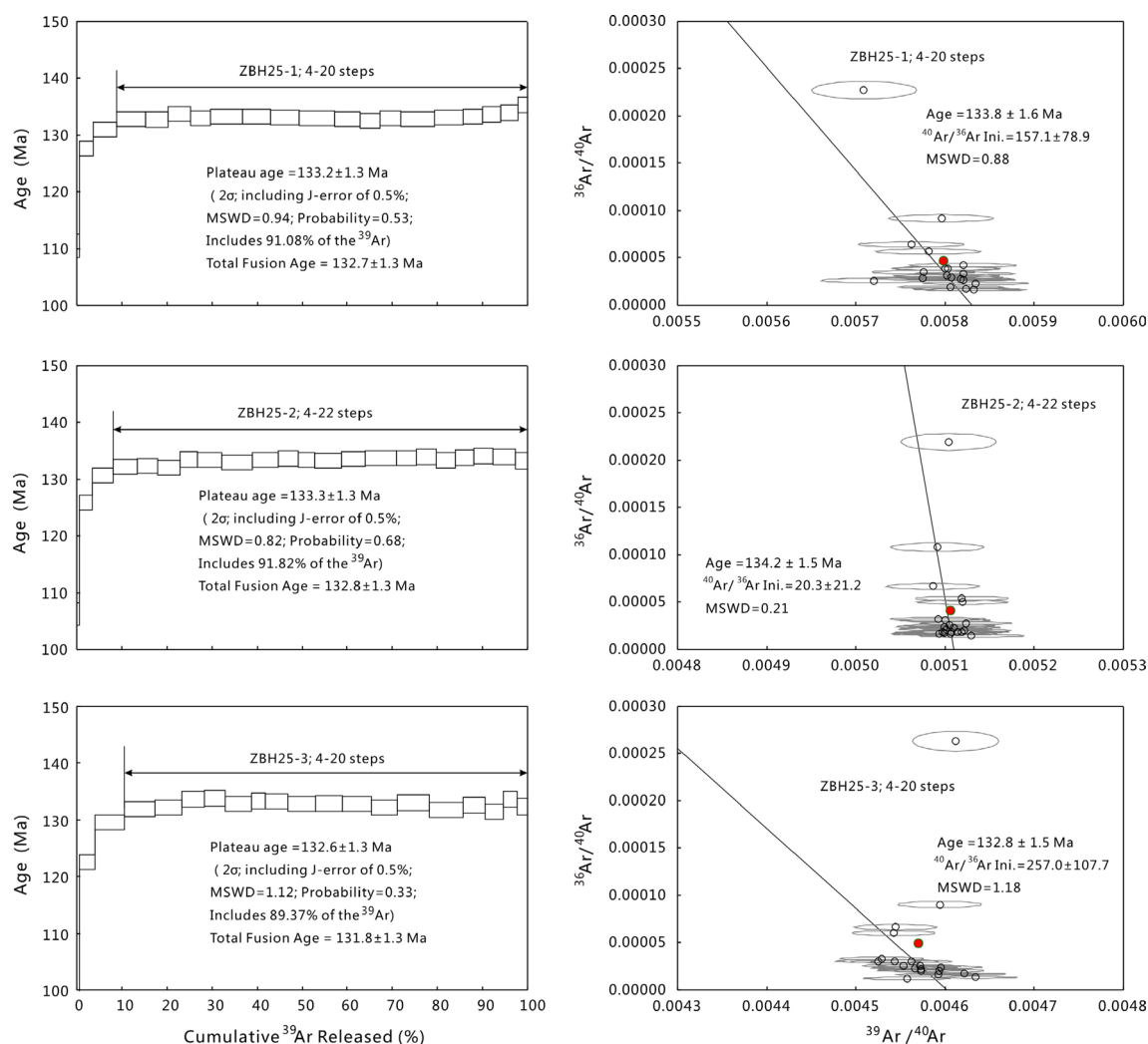


Fig. 11 The $^{40}\text{Ar}/^{39}\text{Ar}$ step-heating spectra and inverse isochrons for ZBH25. The box heights on the plateau diagram represent the 2σ uncertainties for each step

factors between YBCs and FCs (RYBCs FCs = 1.044296 ± 0.003968 , Wang et al. 2014), the recommended age of YBCs should be 29.547 ± 0.206 Ma based on FCs age of Renne et al. (2011). Our analytical result is consistent with the established age and its uncertainty is slight improvement on previously published data.

ZBH25 biotite was separated from Fangshan granodiorite complex in the southwest of Beijing, China. It was developed for K–Ar and $^{40}\text{Ar}/^{39}\text{Ar}$ age determination, and it is used to calculate J-values during irradiation in some laboratories in China. The K–Ar age is 132.9 ± 1.3 Ma and the calibrated $^{40}\text{Ar}/^{39}\text{Ar}$ age of ZBH25 is 133.0 ± 0.3 Ma relative to a Ga1550 age of 98.8 Ma (Sang et al. 2006). Detailed laser step-heating experiments of 20–22 steps were conducted on three aliquots of ZBH25 biotite (Fig. 11, denoted ZBH25-1 to ZBH25-3). These analyses showed age spectrums with increasing ages in the three lowest temperature steps followed by 17–19 stable age steps and yielded integrated ages of $132.6\text{--}133.3 \pm 1.3$ Ma for 89.4%–91.1% of ^{39}Ar released (2σ , probability = 0.33–0.68, MSWD = 0.82–1.12, TFA = $131.8\text{--}132.8 \pm 1.3$ Ma) and a weighted mean age of 133.0 ± 0.76 Ma (2σ). The age coincides with the published value, and its uncertainty is at the same level.

6 Summary

We have established a $^{40}\text{Ar}/^{39}\text{Ar}$ dating system based on a Nu instruments Noblesse mass spectrometer and a CO_2 laser heating apparatus at IGCAS. The system was configured to accurately and precisely date small masses of minerals and volcanic rocks. Five aliquots of Alder Creek sanidine produced ages ranging from 1.174 ± 0.012 to 1.181 ± 0.013 Ma and a weighted mean age of 1.176 ± 0.006 Ma (2σ). Four Bern4M aliquots produced ages of $18.66 \pm 0.19\text{--}18.85 \pm 0.19$ Ma and a weighted mean age of 18.75 ± 0.16 Ma (2σ). Five YBCs aliquots yielded ages ranging from 29.39 ± 0.29 to 29.60 ± 0.30 Ma and a weighted mean age of 29.50 ± 0.19 Ma (2σ). Three aliquots ZBH25 gave ages of $132.6 \pm 1.3\text{--}133.3 \pm 1.3$ Ma and a weighted mean age of 133.0 ± 0.76 Ma (2σ). The results overlap the established age of these mineral standards and the analytical uncertainties are at the same level with those of the foremost Ar/Ar laboratories world-wide.

Acknowledgements We are very grateful to Huaiyu He, Wenbei Shi, Liekun Yang (Institute of Geology and Geophysics, CAS) and Xiujuan Bai (China University of Geosciences, Wuhan) for helpful advice and John Saxton, Bo Gao (Nu instrument) for technical support. We thank Fei Wang and Huaning Qiu (reviewers) for their constructive comments. This study was jointly funded by The

National Key R&D Program of China (2016YFC0600405) and The National Natural Science Foundation of China (Grant No. 40903022).

References

- Bai XJ, Qiu HN, Liu WG, Mei LF (2018) Automatic $^{40}\text{Ar}/^{39}\text{Ar}$ dating techniques using multicollector ARGUS VI noble gas mass spectrometer with self-made peripheral apparatus. *J Earth Sci*. <https://doi.org/10.1007/s12583-017-0948-9>
- Coble MA, Grove M, Calvert AT (2011) Calibration of Nu-Instruments Noblesse multicollector mass spectrometers for argon isotopic measurements using a newly developed reference gas. *Chem Geol* 290:75–87
- Cosca M (2007) $^{40}\text{Ar}/^{39}\text{Ar}$ geochronology by multicollector mass spectrometry. EOS Transactions of the American Geophysical Union 88 Fall Meeting Suppl., Abstract V32B-05
- Hall CM, Walter RC, Westgater JA (1984) Geochronology, stratigraphy and geochemistry of Cindery Tuff in Pliocene hominid-bearing sediments of the Middle Awash, Ethiopia. *Nature* 308:26–31
- Ireland TR (2013) Recent developments in isotope-ratio measurements for geochemistry and cosmochemistry. *Rev Sci Instrum* 84:011101. <https://doi.org/10.1063/1.4765055>
- Jicha B, Sobol P, Singer BS (2010) The UW-Madison 5-collector mass spectrometer for high-precision $^{40}\text{Ar}/^{39}\text{Ar}$ geochronology. EOS Transactions of the American Geophysical Union 91 Fall Meeting Suppl., Abstract V31A-2299
- Jicha BR, Singer BS, Sobol P (2016) Re-evaluation of the ages of $^{40}\text{Ar}/^{39}\text{Ar}$ sanidine standards and supereruptions in the western US using a Noblesse multi-collector mass spectrometer. *Chem Geol* 431:54–66
- Kim J, Jeon S (2015) $^{40}\text{Ar}/^{39}\text{Ar}$ age determination using ARGUS VI multiple-collector noble gas mass spectrometer: performance and its application to geosciences. *J Anal Sci Technol* 6:4. <https://doi.org/10.1186/s40543-015-0049-2>
- Koppers AAP (2002) ArArCALC-software for $^{40}\text{Ar}/^{39}\text{Ar}$ age calculations. *Comput Geosci UK* 28:605–619
- Kuiper KF, Deino A, Hilgen FJ, Krijgsman W, Renne PR, Wijbrans JR (2008) Synchronizing rock clocks of earth history. *Science* 320:500–503. <https://doi.org/10.1126/science.1154339>
- Lee JY, Marti K, Severinghaus JP, Kawamura K, Yoo HS, Lee JB, Kim JS (2006) A redetermination of the isotopic abundances of atmospheric Ar. *Geochim Cosmochim Acta* 70:4507–4512
- Mark DF, Barfod D, Stuart FM, Imlach J (2009) The ARGUS multicollector noble gas mass spectrometer: Performance for $^{40}\text{Ar}/^{39}\text{Ar}$ geochronology. *Geochem Geophys Geosyst*. <https://doi.org/10.1029/2009gc002643>
- Marrocchi Y, Burnard PG, Hamilton D, Colin A, Pujol M, Zimmermann L, Marty B (2009) Neon isotopic measurements using high-resolution, multicollector noble gas mass spectrometer: HELIC-MC. *Geochem Geophys Geosyst*. <https://doi.org/10.1029/2008GC002339>
- McDougall I, Harrison TM (1999) Geochronology and thermochronology by the $^{40}\text{Ar}/^{39}\text{Ar}$ method, 2nd edn. Oxford University Press, Oxford, pp 1–267
- Merrillue C, Turner G (1966) Potassium-argon dating by activation with fast neutrons. *J Geophys Res* 71:2852–2857
- Niespolo EM, Rutte D, Deino AL, Renne PR (2017) Intercalibration and age of the Alder Creek sanidine $^{40}\text{Ar}/^{39}\text{Ar}$ standard. *Quat Geochronol* 39:205–213
- Phillips D, Matchan EL (2013) Ultra-high precision $^{40}\text{Ar}/^{39}\text{Ar}$ ages for Fish Canyon Tuff and Alder Creek Rhyolite sanidine: new

- dating standards required? *Geochim Cosmochim Acta* 121:229–239
- Phillips D, Matchan EL, Honda M, Kuiper KF (2017) Astronomical calibration of $^{40}\text{Ar}/^{39}\text{Ar}$ reference minerals using high-precision, multi-collector (ARGUS VI) mass spectrometry. *Geochim Cosmochim Acta* 196:351–369
- Renne PR, Swisher CC, Deino AL, Karner DB, Owens TL, DePaolo DJ (1998) Intercalibration of standards, absolute ages and uncertainties in $^{40}\text{Ar}/^{39}\text{Ar}$ dating. *Chem Geol* 145:117–152
- Renne PR, Balco G, Ludwig KR, Mundil R, Min K (2011) Response to the comment by W.H. Schwarz et al. on “Joint determination of ^{40}K decay constants and $^{40}\text{Ar}/^{40}\text{K}$ for the Fish Canyon sanidine standard, and improved accuracy for $^{40}\text{Ar}/^{39}\text{Ar}$ geochronology” by P.R. Renne et al. (2010). *Geochim Cosmochim Acta* 75:5097–5100
- Rivera TA, Storey M, Zeeden C, Hilgen FJ, Kuiper K (2011) A refined astronomically calibrated $^{40}\text{Ar}/^{39}\text{Ar}$ age for Fish Canyon sanidine. *EPSL* 311:420–426
- Rivera TA, Storey M, Schmitz MD, Crowley JL (2013) Age intercalibration of $^{40}\text{Ar}/^{39}\text{Ar}$ sanidine and chemically distinct U/Pb zircon populations from the Alder Creek Rhyolite Quaternary geochronology standard. *Chem Geol* 345:87–98
- Sang HQ, Wang F, He HY, Wang YL, Yang LK, Zhu RX (2006) Intercalibration of ZBH-25 biotite reference material utilized for K-Ar and $^{40}\text{Ar}/^{39}\text{Ar}$ age determination. *Acta Petrol Sin* 22:3059–3078 (**in Chinese with English Abstract**)
- Turrin BD, Swisher CC III (2010) Mass discrimination monitoring and intercalibration of dual collectors in noble gas mass spectrometer systems. *Geochem Geophys Geosyst.* <https://doi.org/10.1029/2009gc003013>
- Wang F, Jourdan F, Lo CH, Nomade S, Guillou H, Zhu RX, Yang LK, Shi WB, Feng HL, Wu L, Sang HQ (2014) YBCs sanidine: a new standard for $^{40}\text{Ar}/^{39}\text{Ar}$ dating. *Chem Geol* 388:87–97
- Zhang XD, Honda M, Hamilton D (2016) Performance of the high resolution, multi-collector helix mc plus noble gas mass spectrometer at the Australian National University. *J Am Soc Mass Spectrom* 27:1937–1943